Journal of the European Ceramic Society 19 (1999) 2233–2239

PII: S0955-2219(99)00105-3
0955-2219/99/$ - see front matter

Modeling of Thermal Explosion in Constrained Dies for B_4C–Ti and BN–Ti Powder Blends

M. Shapiro, [a]* I. Gotman [b] and V. Dudko [a]

[a]Laboratory of Transport Processes in Porous Materials, Faculty of Mechanical Engineering, Technion — Israel Institute of Technology, Haifa 32000, Israel
[b]Faculty of Materials Engineering, Technion — Israel Institute of Technology, Haifa 32000, Israel

Abstract

The process of reactive in-situ synthesis of dense particulate reinforced TiB_2/TiC and TiB_2/TiN ceramic matrix composites from B_4C–Ti and BN–Ti powder blends with and without the addition of Ni has been modeled. The objective of modeling was the determination of optimal thermal conditions preferable for production of fully dense ceramic matrix composites. Towards this goal heat transfer and combustion in dense and porous ceramic blends were investigated during heating at a constant rate. This process was modeled using a heat transfer–combustion model with kinetic parameters determined from the differential thermal analysis of the experimental data. The kinetic burning parameters and the model developed were further used to describe the process of combustion synthesis in a constrained die under pressure. It has been shown that heat removal from the reaction zone affects the ignition temperature of thermal explosion. © *1999 Elsevier Science Ltd. All rights reserved.*

Keywords: BN, B_4C, modelling, thermal explosion, composites.

1 Introduction

One of the major factors restricting the widespread use of high performance ceramics for advanced structural applications is the difficulty of producing dense components from these materials. Furthermore, the toughening of the inherently brittle ceramics via the composite approach, i.e. incorporation of a second phase into a ceramic matrix, dramatically increases the difficulty and expense of the material processing. In recent years, the concept of in-situ ceramic matrix composites (CMCs) — materials in which desired reinforcements and matrices are formed during processing, has become increasingly important as an attractive alternative route to cost-effective ceramic-based structures.

Self-propagating high-temperature synthesis (SHS), or combustion synthesis, is one of the rapidly emerging technologies used to synthesize in-situ refractory ceramic materials.[1–5] The principle of this technique is that initial reagents, when ignited, spontaneously transform into products due to the exothermic heat of reaction. An inherent limitation of combustion synthesis is the high retained porosity of the synthesized products. It has been demonstrated that application of pressure during or subsequent to the combustion step can considerably increase the product density.[5–10] Two general SHS modes have been recognized: combustion wave propagation and volumetric combustion, or thermal explosion.

The thermal explosion mode of the SHS process is much less studied than the combustion wave mode. This is even more true regarding thermal explosion in constrained molds under pressure. As for any SHS process, the ignition and the combustion temperature of thermal explosion are strongly affected by the heat transfer to and from the reaction zone. When a reagent powder blend is placed in a die, the heat transfer rate depends not only on the thermal conductivity and specific heat of the reagents and products, but also on the thermophysical properties of the die material and on the initial die temperature. The roles of these latter factors as a means of controlling the thermal explosion process are still not fully assessed.

*To whom all correspondence should be addressed. Fax: +972-4-832-4533; e-mail address: mersm01@techunix.technion.ac.il

Table 1. Experimental data on specimens tested

Specimen	*Material*	*Density* ($kg\ m^{-3}$)	*Porosity* (%)	*Kinetic coefficients* k_1 (s^{-1})	*Kinetic coefficients* k_2	*Thermal conductivity* ($W\ m^{-1}K^{-1}$)	*Heat rate* ($°C\ min^{-1}$)
N1 in air	2BN + 3Ti	3630	< 1	19 500	0·1	5·0[1a]	20
C1 in air	B_4C + 3Ti	3700	< 1	24 500	0·1	4·0[a]	20
N2 in air	2BN + 3Ti	3200	12	160	0·1	9·0[a]	20
C2 in air	B_4C + 3Ti	2940	20	23 000	0·1	3·2[a]	20
NN1 in Ar	2BN + 3Ti + 1·5Ni	3800	15	6000	0·1	7·5[b]	20
NN2 in Ar	2BN + 3Ti + 1·5Ni	3800	15	6000	0·1	7·0[b]	20
NN3 in Ar	2BN + 3Ti + 1·5Ni	3800	15	6500	0·1	7·5[b]	20
NN4 in Ar	2BN + 3Ti + 0·95Ni	4000	5	8500	0·1	5·2[b]	20
NN5 in Ar	2BN + 3Ti + 0·95Ni	4000	5	8000	0·1	6·0[b]	10
CN1 in Ar	B_4C + 3Ti + 0·95Ni	3300	22	2000	0·1	2·0[b]	20
CN2 in Ar	B_4C + 3Ti + 0·95Ni	3300	22	340 000	0·1	2·0[b]	10

[a] At 600 K.
[b] At 525 K.

The specific objective of this paper is to identify and investigate the optimal thermal conditions required for the fabrication of dense TiB_2/TiN and TiB_2/TiC CMCs from BN–Ti and B_4C–Ti powder blends via thermal explosion in constrained molds under pressure. Towards this goal heat transfer and combustion in dense and porous ceramic blends are investigated during heating at a constant rate. The apparent thermal diffusivity is measured during heating, together with the characteristic temperature drop across the specimen. The process is modeled using a heat transfer-combustion model with kinetic burning parameters determined from the differential thermal analysis of the data obtained on the experimental temperature profiles. The kinetic burning parameters and the model developed are further used to describe combustion synthesis in a constrained die under pressure. It is shown that heat removal from the reaction zone affects the ignition temperature of thermal explosion.

2 Measurement of Thermophysical Properties

The composition and properties of the starting specimens experimentally tested in the present work are summarized in Table 1. SHS reactions that take place in these powder blends and the corresponding adiabatic temperatures, T_{ad}, calculated at the preheating temperature, T_0, of 1000°C are given in Table 2. The high values of T_{ad} indicate the possibility of SHS in all the compositions studied.

The properties of dense specimens and non-dense compacts which were experimentally tested are summarized in Table 1. Figure 1 presents a schematic of the measurement cell with a specimen placed within a steel 304 container. The diameter d and the length l of the specimens varied in the following ranges: $d = 18-20$ mm, $l = 40 \pm 1$ mm. The non-dense

Table 2. SHS reactions for the specimens tested, and the corresponding adiabatic temperatures, T_{ad} calculated at the preheating temperature of 1000°C

Reaction	*Calculated* T_{ad} *(K) (at* $T_0 = 1000°C$*)*
$B_4C + 3Ti \rightarrow TiB_2 + TiC$	3223
$B_4C + 3Ti + 0{\cdot}95Ni \rightarrow 2TiB_2 + TiC + 0{\cdot}95Ni$	3192[a]
$2BN + 3Ti \rightarrow TiB_2 + 2TiN$	3192[a]
$2BN + 3Ti + 1{\cdot}5Ni \rightarrow TiB_2 + 2TiN + 1{\cdot}5Ni$	2867
$2BN + 3Ti + 0{\cdot}95Ni \rightarrow TiB_2 + 2TiN + 0{\cdot}95Ni$	3002

[a] T_m of TiB_2.

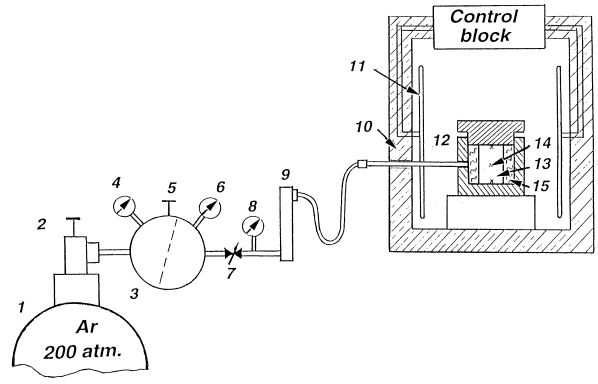

Fig. 1. Experimental setup: 1, argon container; 2, valve; 3, pressure reducer; 4, 6, 8, manometers; 5, reducing valve; 7, flow rate control valve; 9, flowmeter; 10, furnace; 11, heater; 12, measurement cell; 13, specimen; 14, thermocouples; 15, insulation.

compacts were consolidated from powder blends at 1·5 to 2·2 GPa, and the dense (≥ 95% TD) samples were cold sintered[11] at 3 GPa. The specimens were placed in the container between the plate and the lid, both of which were in a good thermal contact with the specimen. The container was put vertically in the furnace and heated from the sides (see Fig. 1). This arrangement was used for measurements of dense samples (with porosity of < 1%).

We examined the nonstationary temperature field in the specimens and found out that the tem-

perature in the upper point is always higher than in the lowermost point. This introduced inaccuracy in the measurement method, which cannot be taken into account in the calculations of thermal conductivity.

The above shortcoming does not exist in the measurement cell which was developed later for porous specimens (with porosity of about 20%). This cell is placed horizontally in the furnace, so that the heating occurs from the lids. The exact position of the cell within the furnace was determined to assure that the temperature field within the samples is symmetric. During the measurement of thermal diffusivity, argon was constantly supplied in a way that ensured the specimen was not in contact with air. Argon was discharged from the openings within the container, the sizes of which, as well as the permeability of the porous insulator, were chosen to create the necessary hydraulic resistance for the flowing argon. The Ar flow rate was chosen to make the temperature of the gas supplied to the cell as close as possible to the temperature of the lateral surface of the specimen. For this purpose the temperature of argon entering the measurement cell was monitored using a special thermocouple.

The experimental method for the determination of thermal conductivity and thermal diffusivity is described elsewhere.[12,13] The measurement cell for testing the samples in the argon atmosphere was calibrated using the steel 304 specimen of the same size as the ceramic specimens. The results on thermal conductivity versus temperature were compared with the literature data. The discrepancy did not exceed 5%.

3 Experimental Results

Figure 2 depicts one of the typical results for thermal conductivity of compacted powder blends. One can see that k significantly increases at high temperatures due to the combustion reaction. In this temperature range the measurements do not represent the true material properties, but rather depend on the reaction kinetics. The values of k at lower temperatures are less affected by the combustion process, where they depend on the porosity and the contact area between powder particles. As a general trend, the conductivity decreases with increasing porosity and decreasing contact area between powder particles, which depends on the consolidation pressure.

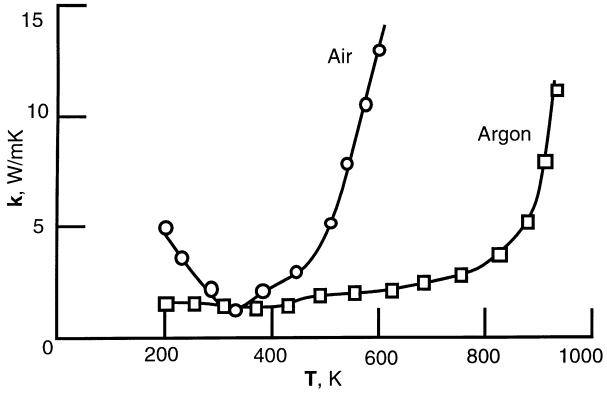

Fig. 2. Thermal conductivity of ($B_4C + 3Ti$) specimens versus temperature in air and argon.

When measured in air, the thermal conductivity of C2 specimen exhibited the occurrence of an exothermic reaction at temperature of $\sim$600°C, which is significantly lower than the experimentally observed ignition temperature of thermal explosion of the $B_4C + 3Ti$ blend ($T_{ig} \approx 950$°C[14,15]). Apparently, this is due to the heat release resulting from the reaction with surrounding air. This trend repeated itself for all specimens tested with porosity of 20% and above. To avoid this unwanted effect, further tests were conducted in an argon atmosphere. In this case, the measurements performed for a similar specimen C3 showed that the exothermic reaction begins at a much higher temperature ($\geq$ 800°C) than for the similar specimen in air.

These tests revealed also a significant difference between the thermal diffusivity of B_4C–Ti–Ni specimens in argon and in air at low temperatures (about 200°C), which amounts up to the factor of 8. This cannot be attributed to the difference between thermal conductivities of these gases, which is not large enough to explain this trend. Apparently, the larger values of k measured in air are a result of the heat released during the oxidation reaction, occurring as early as 200°C.

In addition, the difference between the temperatures of thermocouples 1, 2, 3 within the specimen was used to determined the kinetic coefficients of the combustion process (see below).

4 Theoretical Model

The lumped-capacity theoretical model has been developed and aimed at describing the combustion process and determination of the kinetic parameters characterizing the combustion kinetics. This model is schematically shown in Fig. 3.

The specimen's mass is divided into two parts: one corresponding to the central part, with the temperature T_2 and a surface layer with the temperature T_1 both measured by thermocouples. The thermal resistance between the layers is $(A_1h_1)^{-1}$, where A_1 is the cross-section area and $h_1 = k_1/\Delta_x$ is the heat transfer coefficient, expressed via the specimen's thermal conductivity and the distance between

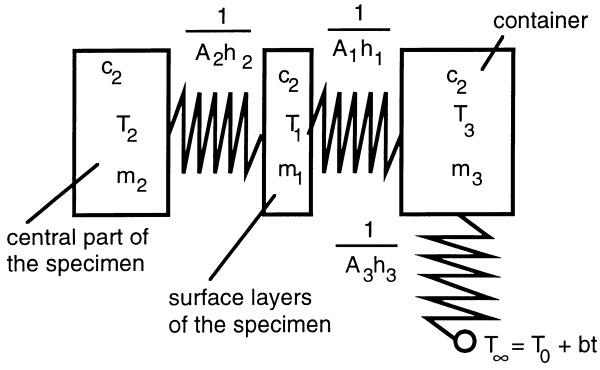

Fig. 3. Schematic of the lumped-capacity heat transfer and combustion model.

thermocouples Δ_x. The surface layer exchanges heat also with the container via the corresponding thermal resistance $(A_2h_2)^{-1}$, wherein h_2 takes into account the contact resistance and thermal conductivity of the container material (steel 304). The container in turn, is heated via thermal resistance $(A_3h_3)^{-1}$ within the furnace wherein the temperature changes linearly with time $T_\infty = T_0 + bt$, with b being the heating rate.

According to the above model the equations of the evolution of the temperatures are:

$$c_1m_1\frac{\mathrm{d}T_1(t)}{\mathrm{d}t} = V_1Q\exp\left(-\frac{E}{RT_1(t)}\right)\kappa(\sigma_1) - A_1h_1[T_1(t) - T_3(t)] - A_2h_2[T_1(t) - T_2(t)], \quad (1)$$

$$c_2m_2\frac{\mathrm{d}T_2(t)}{\mathrm{d}t} = V_2Q\exp\left(-\frac{E}{RT_2(t)}\right)\kappa(\sigma_2) - A_2h_2[T_2(t) - T_1(t)], \quad (2)$$

$$c_3m_3\frac{\mathrm{d}T_3(t)}{\mathrm{d}t} = A_1h_1[T_3(t) - T_1(t)] - A_3h_3[T_3(t) - T_o - bt], \quad (3)$$

where V_1, c_1 V_2, c_2 are the volumes and the specific heats of the corresponding parts of the specimen, T_o is the initial temperature, Q is the volumetric heat release, E is the activation energy, R is the gas constant and κ is the combustion kinetic function, dependent on the volumetric concentrations (of any of the components), σ_1, σ_2 within the layers. The equation for evolution of σ_1, σ_2 are:

$$\frac{\mathrm{d}\sigma_i(t)}{\mathrm{d}t} = \sigma_i(t)\exp\left(-\frac{E}{RT_i(t)}\right)\kappa(\sigma_i), \quad i = 1, 2 \quad (4)$$

wherein the function κ is

$$\kappa[\sigma_i(t)] = \frac{k_1}{k_2[\sigma_i(0) - \sigma_i(t)]^{1/3} + 1}, \quad (5)$$

In the above, the kinetic constants k_1, k_2 are unknown quantities, which are determined from the differential thermal analysis of the experimental data, namely, by analyzing the temperature difference $T_1 - T_2$.

The physical reason underlying the functional dependence (eqn 5) may be outlined as follows. Suppose that initially, i.e. before combustion, the initial reaction rate κ is determined by a time constant α_1, i.e. $\kappa \sim 1/\alpha_1$. When the combustion reaction begins, the reaction rate diminishes because of the formation of the product layer separating any two reagent particles. The reaction rate is thus determined jointly by the thickness δ_i of this layer, which increases with time, as the reaction progresses. As such one can express the reaction rate in the form

$$\kappa \sim \frac{1}{\alpha_2\delta_i(t) + \alpha_1},$$

where α_2 is a (time-independent) constant. The thickness $\delta_i(t)$ of the product layer may be expressed via the volumetric concentrations in the form $\delta_i(t) \sim V[\sigma_i(0) - \sigma_i(t)]^{1/3}$, where V is the total volume of the product. Introducing this formula into the above expression for the reaction rate and renormalizing the terms in the denominator one obtains formula (eqn 5) with constants k_1, k_2 expressible via α_1, α_2 and V.

Equations (1)–(5) were solved subject to the initial conditions

$$\sigma_i(0) = 1, i = 1, 2, \quad T_i(0) = T_0, i = 1, 2, 3. \quad (6)$$

As a result, we determine the temperature difference $T_1 - T_2$ as a function of time, which was used to describe the comparable data measured in the experiments. The calculations were performed for different k_1, k_2, which were chosen so as to provide the best agreement with the measured values of the temperature difference throughout the combustion process.

5 Results

The model was used in a two-fold manner. First the calculations were performed for the differential thermal analyses and estimations of the kinetic coefficients. At the next stage we used the fitted values of k_1, k_2 to calculate the behavior of the specimens undergoing the thermal explosion in a constrained die.

The results of differential thermal analysis are presented in Table 1 and in Fig. 4. which shows the typical calculated curves for T_1-T_2 and the experimental points for the same quantity. The coefficient k_1 describes the reaction rate at the beginning of the burning process, when the difference $\sigma_i(0) - \sigma_i(t)$ is small and the kinetics of burning is in its fastest stage [see eqn (5)].

One can see that k_1 is larger for dense samples, wherein the reagent particles are more densely packed against each other and the contact area is the largest (see Table 1). The coefficient k_2 describes the impediment of burning, incurred by the formation of the barrier layer of reaction products between the reagent particles. It is seen to be largely independent of the specimen porosity (see Table 1).

One general trend may be observed from the data on the kinetic coefficients shown in Table 1. The kinetic coefficients obtained from the Differential Thermal Analyses of similar specimens heated in the air exhibit a significant difference (e.g. N1 and N2). This may be attributed to the difference in porosities of the specimens. The larger porosity of specimen N2 triggers the oxidation reaction which affects the values of the kinetic coefficient k_1. Moreover this reaction diminishes the temperature gradient within the specimen even at temperatures of about 600 K, for which thermal conductivity was determined. Accordingly, the experimental value of thermal conductivity for a more porous specimens N2 had been obtained larger than that for its denser counterpart N1. The values of the kinetic coefficient k_1 obtained from the data on the identical specimens collected in argon have better reproducibility, save the unrealistically large value of k_1 for specimen CN2.

The values of k_1, k_2 listed in Table 1 were used to model the SHS process. For this purpose we used the model analogous to the models in Refs[1–6], with the following changes:

1. the temperatures within the specimen were calculated, in conditions when it is heated by the die;
2. the temperature of the die was calculated assuming that its outer surface is held at a constant temperature (e.g. 1300 K or else);
3. the values of the kinetic coefficients determined from the differential thermal analyses retain their values also in a constrained die under pressure.

Examples of the results of such calculations for the 2BN + 3Ti specimen (N1) is shown in Fig. 5(a)–(c). Explicitly, Fig. 5(a) shows the evolution of temperature within the specimen placed instantaneously in the die whose temperature is held at 1300 K. The character of the temperature curves shows that thermal explosion does not occur in these conditions, as predicted by the model when using activation energy $E = 150$ KJ/mole. Fig. 5(a) also shows the effect of the activation energy on thermal explosion. One can see that with E diminished from 150 to 80 KJ mole^{-1} the ignition occurs after about 35 s, which qualitatively agrees with the comparable time period measured for thermal explosion under pressure in the $B_4C + 3Ti$ blend.[14,15]. Fig. 5(b) shows the influence of the initial die temperature on thermal explosion. One can see that ignition occurs beginning from $T_{die} \approx 1620$ K, whereas lower initial temperatures do not lead to SHS. Finally Fig. 5(c) exhibits the effect of chemical composition on SHS. One can see that the addition of Ni promotes thermal explosion, presumably due to the formation of the low-melting Ti–Ni eutectic phase.[16] Although this process does not explicitly appear in the model, its influence is implicitly accounted for within the kinetic coefficients.

The values of the kinetic constants k_1, k_2 were determined for $E = 150$ KJ mole^{-1}. Therefore, the use of the lower value for E necessitates re-calculation of k_1, k_2. Rather than doing so for $E = 80$ KJ mole^{-1}, which appears rather low, we returned to the previous activation energy $E = 150$ KJ mole^{-1} and calculated the value of k_1 which corresponds to the threshold of ignition. This was done for the fixed value of k_2 and for various values of thermal conductivity of the die material, k_{die}. As a result, we obtained the threshold value $(k_1)_{ignition}$. For the thermal conductivity of Ni-based superalloy M-6000 ($\sim$ 16 W m^{-1}K^{-1}) $(k_1)_{ignition}$ is close to 10^8 s^{-1}. The calculations show that reducing the die material (M-6000) thermal conductivity assists the SHS process on its later stages (after ignition).*

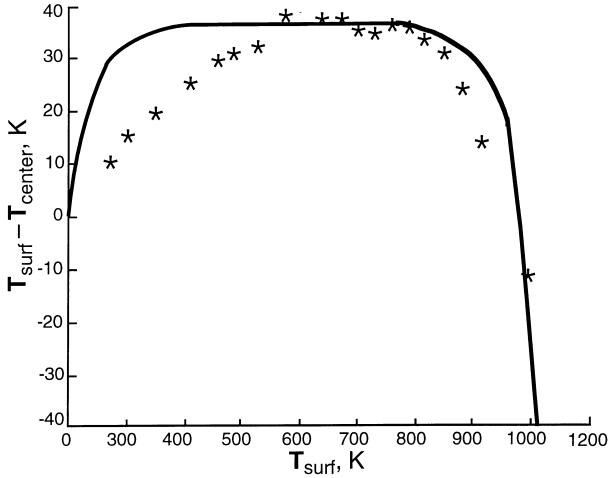

Fig. 4. Determination of kinetic combustion constants of the (2BN + 3Ti + 1·5Ni) specimen (NN1) by the differential thermal analysis: $k = 7{\cdot}5$ W mK^1, $\rho = 3800$ kg m^{-3}, $k_1 = 6000$ s^{-1}, $k_2 = 0{\cdot}1$.

*More quantitative conclusions about the complicated specimen's thermal balance during heating in the die can be reached on the basis of the differential heat transfer model (see below).

Still several-fold decrease of k_{die} yielded lower $(k_1)_{ignition}$, which was however still larger than k_1 determined from the differential thermal analyses. As such, the lumped capacity model predicts that if a specimen does not ignite in the existing die, it will not ignite in other thermal conditions. This was found both for $B_4C + 3Ti$ and $2BN + 3Ti$ specimens.

The above conclusion is inconsistent with the observations of the SHS process for several specimens tested. This pointed to the possibility that the kinetic constants were determined inadequately from the differential thermal analyses. To check this possibility, we calculated the threshold value $(k_1)_{ignition}$ in a wide range of kinetic parameters k_2. Some results of these calculations are depicted in Fig. 6 (white symbols), together with the values of k_1, which most closely fit the differential thermal analysis data for each given k_2 (filled symbols). One can see that for values of k_2 exceeding 10 there is a large gap between these two sets of data. On the other hand, for k_2 less than 1, these two predictions agree satisfactorily. Therefore, the values of k_2 determined from DTA are unrealistically large. The determination of the optimum values of the kinetic coefficients should be focused at the range where k_2 is much smaller. Based on the conjecture that the true values of the kinetic constants are in the range of $k_2 = 0{\cdot}1–1$, we can conclude that the specimen C2 ($B_4C + 3Ti$) is likely to ignite, since in this range the calculated threshold values of k_1 and those determined from the DTA are close to each other.

On the other hand, similar data for N2 specimen (not shown) imply that even in the range of small k_2 there is a significant gap between the calculated threshold values of k_1 and those determined from the DTA. Therefore, according to the model, this specimen will not ignite.

The above conclusions are summarized in Table 3, which includes also the conditions at which the calculations were performed and experimental observations of thermal explosion under pressure.[14–16] Basing on the value of the activation energy $E = 150$ KJ mole^{-1}, one can see that the proposed model can adequately predict the ignition of thermal explosion in a constrained die. The lowermost ignition temperature for the $2BN + 3Ti$ (N2) porous sample obtained from calculations is 1625 K, as opposed to 1525 K, which was measured for thermal explosion in a constrained die.[16] This difference may be partially attributed to the inaccuracy in determination of the kinetic coefficients for the porous samples in air, where low temperature oxidation

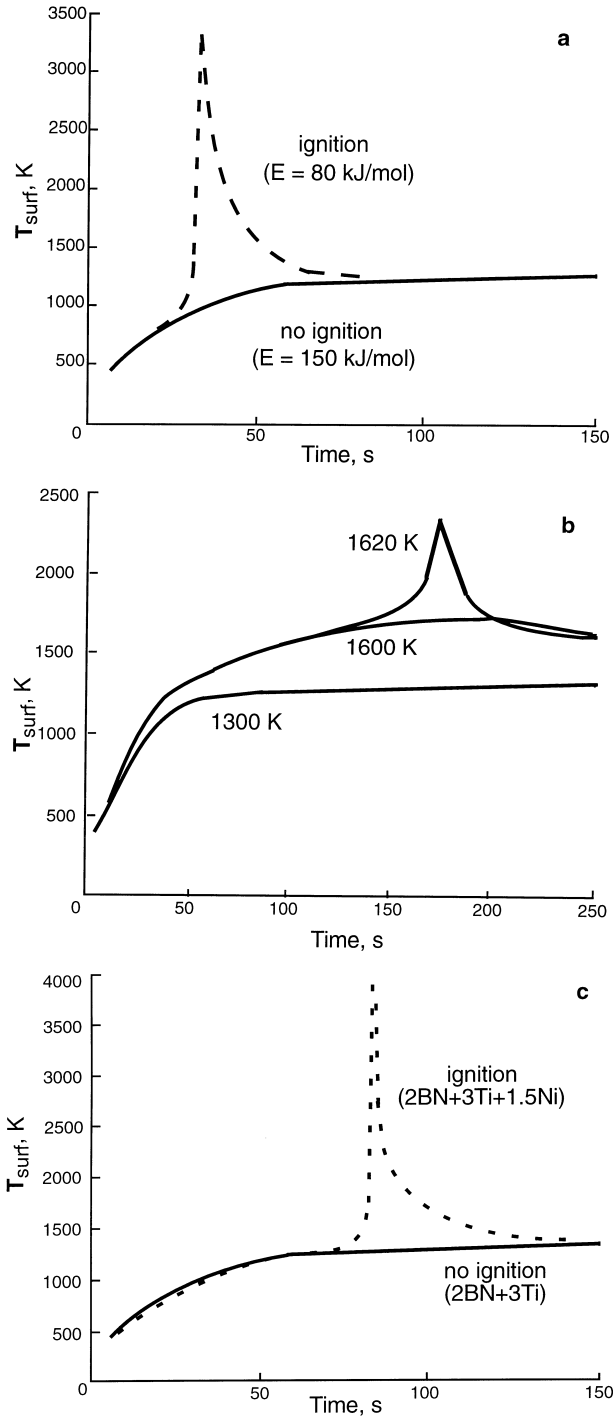

Fig. 5. Modeling of thermal explosion in $(2BN + 3Ti)$ and $(2BN + 3Ti + 1{\cdot}5Ni)$ specimens: a, the effect of activation energy, E, at $T\infty = 1300$ K; b, the effect of temperature within the die, for $E = 150$ KJ mole^{-1}, minimal $T_{ig} = 1620$ K; c, the effect of chemical composition at $T_\infty = 1300$ K.

Table 3. Summary of ignition events, as occurred in the experiment and predicted by the model

Specimen	*Thermal explosion in the die (experiment)*	*Theoretical model* E = *150 KJ mol*$^{-1}$	*Theoretical model* E = *200 KJ mol*$^{-1}$	T∞ (T$_{die}$)
N2	No ignition	No ignition	No ignition	1300
N2	No ignition	No ignition	No ignition	1385
N2	Ignition	No ignition	No ignition	1525
N2	Ignition	Ignition	No ignition	1620
C2	Ignition	Ignition	Ignition	1300
C2	No ignition	Ignition	No ignition	1100
NN2	Ignition	Ignition	No ignition	1300

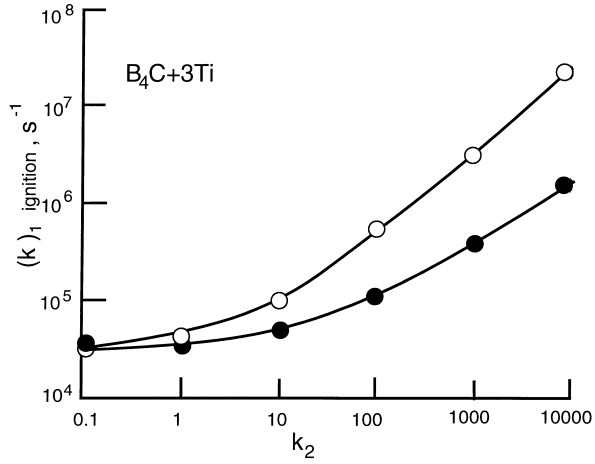

Figure 6. Threshold value of k_1 (hollow symbols), for which the ignition of the ($B_4C + 3Ti$) specimen (C2) occurs, as predicted by the model versus k_2. Black symbols: k_1 versus k_2 obtained from the experimental data. $T_\infty = 1300$ K.

reaction occurs. In contrast, the calculated minimal ignition temperatures for NN2 specimens (tested in argon) was found close to the comparable temperature registered for thermal explosion under pressure.

In passing we will note that this conclusion has recently received an additional support on the basis of calculations performed using a more elaborate differential one-dimensional heat transfer model.[17] This model yields one-dimensional continuous distributions of the temperature and concentration within the specimen and the die for all times. The analysis showed that the latter model in most cases predicts the same ignition (or absence of ignition) events as does the simpler lumped-capacity model, employed for identical specimens and thermal conditions.

6 Conclusions

The process of thermal explosion (SHS) in B_4C–Ti and BN–Ti compacted powder blends can be modeled on the basis of the lumped capacity heat transfer-combustion model. The model hinges on the kinetic burning coefficients which may be experimentally measured by monitoring temperatures within specimens heated with a constant rate. The analyses showed that thermal conditions within the die have a significant effect on the SHS process. These factors may be used as a means of controlling the combustion process and, thereby, the final product properties. Yet a considerable work is needed to determine reliable values of the kinetic constants of various specimens.

Acknowledgement

This research was supported by the Israel Ministry of Science through research grant No. 5864-1-95. VD acknowledges the support of the Gilleady Program for New Immigrant Scientist, Israeli Ministry of Absorption.

References

1. Merzhanov, A. G., Self-propagating high temperature synthesis: twenty years of search and findings. In *Combustion and Plasma Synthesis of High-Temperature Materials*, ed. Z. A. Munir, and J. B. Holt. VCH, New York, 1990, pp. 1–53.
2. Munir, Z. A., Synthesis of high-temperature materials by self-propagating combustion methods. *Ceram. Bull.*, 1988, **67**, 342–349.
3. Munir, Z. A. and Anselmi-Tamburini, U., Self-propagating exothermic reactions the synthesis of high-temperature materials by combustion. *Mater. Sci. Rep.*, 1989, **3**(7–8), 277–365.
4. Holt, J. B., The use of exothermic reactions in the synthesis and densification of ceramic materials. *MRS Bull.*, 1987, **12**, 60–64.
5. Bowen, C. R. and Derby, B., Finite-difference modeling of self-propagating high temperature synthesis of materials. *Acta Metall. Mater.*, 1995, **43**, 3903–3913.
6. Miyamoto, Y., New ceramic processing approaches using combustion synthesis under gas pressure. *Am. Ceram. Soc. Bull.*, 1990, **69**, 686–690.
7. Grebe, H. A., Thadhani, N. N. and Kottke, T., Combustion synthesis and subsequent explosive densification of titanium carbide ceramics. *Metall. Trans.*, 1992, **23A**, 2365–2372.
8. Hoke, D. A. and Meyers, M. A., Consolidation of combustion-synthesized titanium diboride-based materials. *J. Am. Ceram. Soc.*, 1995, **78**, 275–284.
9. LaSalvia, J. C., Meyer, L. W. and Meyers, M. A., Densification of reaction-synthesized titanium carbide by high-velocity forging. *J. Am. Ceram. Soc.*, 1992, **75**, 592–602.
10. Choi, Y., Lee, J. K. and Mullins, E., Densification process of TiC_x–Ni composites formed by self-propagating high-temperature synthesis reaction. *J. Mater. Sci.*, 1997, **32**, 1717–1724.
11. Gutmanas, E. Y., Cold sintering under pressure — mechanisms and application. *Powder Metall. Int.*, 1983, **15**, 129–132.
12. Litovsky, E. and Shapiro, M., Gas pressure and temperature dependencies of thermal conductivity of porous ceramic materials: part 1. Refractories and ceramics with porosity below 30%. *J. Am. Ceram. Soc.*, 1992, **75**, 3425–3439.
13. Litovsky, E., Shapiro, M. and Shavit, A., Gas pressure and temperature dependencies of thermal conductivity of porous ceramic materials: part 2. Refractories with porosity exceeding 30%. *J. Am. Ceram. Soc.*, 1996, **79**, 1366–1376.
14. Olevsky, F., Mogilevsky, P., Gutmanas, E. Y. and Gotman, I., Synthesis of in-situ TiB_2/TiN ceramic matrix composites from dense BN–Ti and BN–Ti–Ni powder blends. *Metall. Mater. Trans.*, 1996, **27A**, 2071–2079.
15. Gotman, I., Travitzky, N. and Gutmanas, E. Y., Dense in situ TiB_2/TiN and TiB_2/TiC ceramic matrix composites: reactive synthesis and properties. *Mater. Sci. Eng.*, 1998, **A244**, 127–137.
16. Gutmanas, E. Y. and Gotman, I., Dense high-temperature ceramics by thermal explosion under pressure. *J. Eur. Ceram. Soc.*, 1999, **19** (13–14), this issue.
17. Shapiro, M., Gotman, I., Matvienko, A. and Dudko, V., Thermal explosion in B_4–Ti and BN–Ti powder blends in restrained dies: measurement of kinetic combustion parameters and modeling. *Int. J. SHS*, 1999, submitted.